

Supplementing Information

Hunting for Advanced High-Energy-Density Materials with Well-Balanced Energy and Safety through Energetic Host–Guest Inclusion Strategy

Yi Wang,¹ Siwei Song,¹ Chuan Huang,¹ Xiujuan Qi,² Kangcai Wang,¹ Yuji Liu,¹ and Qinghua Zhang^{1,*}

*Corresponding Email: qinghuazhang@caep.cn

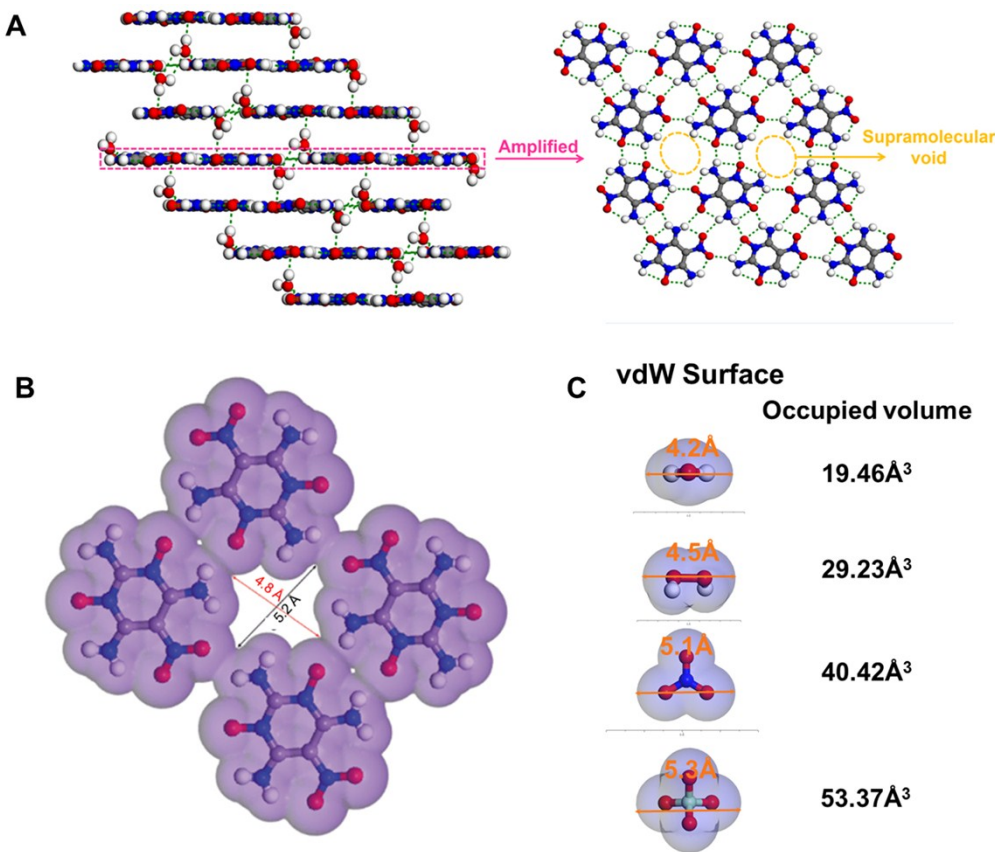


Fig. S1. Crystal structural analysis on ICM-102 monohydrate. (A) 3D crystal structure of ICM-102 monohydrate (left) and 2D molecular sheet of ICM-102 monohydrate in crystal (right), (B) the size of supramolecular void fabricated by four ICM-102 molecules, (C) the sizes of water (H_2O), hydrogen peroxide (H_2O_2), nitrate anion (NO_3^-) and perchloric acid anion (ClO_4^-).

Table S1. Crystallographic data for HGI-1. Single crystal X-ray diffraction data was collected on an Oxford Xcalibur diffratometer with Mo- K_{α} monochromated radiation ($\lambda = 0.71073 \text{ \AA}$). The crystal structures were solved by direct methods.¹ The structures were refined on F^2 by full-matrix least-squares methods using the SHELXTL script package. All non-hydrogen atoms were refined anisotropically.

CCDC	1831628
Formula	C ₄ H ₆ N ₆ O ₄ •0.5H ₂ O ₂
<i>Mr</i>	219.16
Crystal system	monoclinic
Space group	C 2/c
<i>a</i> [Å]	14.128(7)
<i>b</i> [Å]	14.696(8)
<i>c</i> [Å]	7.415(4)
α [°]	90
β [°]	98.866(6)
γ [°]	90
V [Å ³]	1521.1(14)
<i>Z</i>	8
<i>T</i> (K)	100
ρ [g cm ⁻³]	1.914
Mu [mm ⁻¹]	0.174
F(000)	904
θ [°]	2.012 to 27.480
index range	-18 ≤ <i>h</i> ≤ 18 -18 ≤ <i>k</i> ≤ 18 -9 ≤ <i>l</i> ≤ 9
reflections collected	4861
independent reflections	1714 [$R_{\text{int}} = 0.0339$, $R_{\text{sigma}} = 0.0436$]
data/restraints/parameters	1714/14/157
GOF on F ²	1.121
<i>R</i> 1 [I>2σ(I)]	0.0535
<i>wR</i> 2 [I>2σ(I)]	0.1555
<i>R</i> 1(all data)	0.0718
<i>wR</i> 2(all data)	0.1903
largest diff. peak and hole [e Å ⁻³]	0.51/-0.33

Table S2. Crystallographic data for HGI-2. Single crystal X-ray diffraction data was collected on an Oxford Xcalibur diffratometer with Mo- K_{α} monochromated radiation ($\lambda = 0.71073 \text{ \AA}$). The crystal structures were solved by direct methods.¹ The structures were refined on F^2 by full-matrix least-squares methods using the SHELXTL script package. All non-hydrogen atoms were refined anisotropically.

CCDC	1887848
Formula	$\text{C}_4\text{H}_6\text{N}_6\text{O}_4 \cdot \text{HNO}_3$
M_r	265.17
Crystal system	orthorhombic
Space group	Pbca
$a [\text{\AA}]$	11.239(3)
$b [\text{\AA}]$	11.869(3)
$c [\text{\AA}]$	13.511(3)
$\alpha [{}^\circ]$	90
$\beta [{}^\circ]$	90
$\gamma [{}^\circ]$	90
$V [\text{\AA}^3]$	1802.2(7)
Z	8
$T(\text{K})$	173
$\rho [\text{g cm}^{-3}]$	1.955
$\text{Mu} [\text{mm}^{-1}]$	0.184
$F(000)$	1088
$\theta [{}^\circ]$	3.015 to 25.123
index range	-13 $\leq h \leq$ 13 -14 $\leq k \leq$ 13 -16 $\leq l \leq$ 13
reflections collected	12301
independent reflections	1577 [$R_{\text{int}} = 0.0801$, $R_{\text{sigma}} = 0.0507$]
data/restraints/parameters	1577/21/191
GOF on F^2	1.042
$R1$ [$I > 2\sigma(I)$]	0.0447
$wR2$ [$I > 2\sigma(I)$]	0.1137
$R1$ (all data)	0.0625
$wR2$ (all data)	0.1268
largest diff. peak and hole [$e \text{ \AA}^{-3}$]	0.492/-0.295

Table S3. Crystallographic data for HGI-3. Single crystal X-ray diffraction data was collected on an Oxford Xcalibur diffratometer with Mo- K_{α} monochromated radiation ($\lambda = 0.71073 \text{ \AA}$). The crystal structures were solved by direct methods.¹ The structures were refined on F^2 by full-matrix least-squares methods using the SHELXTL script package. All non-hydrogen atoms were refined anisotropically.

CCDC	1887847
Formula	C ₄ H ₆ N ₆ O ₄ HClO ₄
<i>M_r</i>	302.61
Crystal system	orthorhombic
Space group	Pbca
<i>a</i> [\text{\AA}]	12.410(2)
<i>b</i> [\text{\AA}]	9.9590(19)
<i>c</i> [\text{\AA}]	16.305(3)
α [°]	90
β [°]	90
γ [°]	90
V [\text{\AA}³]	2015.2(7)
<i>Z</i>	8
<i>T</i> (K)	173
ρ [g cm ⁻³]	1.995
Mu [mm ⁻¹]	0.439
F(000)	1232
θ [°]	2.99 to 22.48
index range	-14 ≤ <i>h</i> ≤ 15 -12 ≤ <i>k</i> ≤ 12 -20 ≤ <i>l</i> ≤ 12
reflections collected	9864
independent reflections	2146 [$R_{\text{int}} = 0.0800$, $R_{\text{sigma}} = 0.0600$]
data/restraints/parameters	2146/1/176
GOF on F^2	1.045
<i>R</i> 1 [I > 2σ(I)]	0.0456
<i>wR</i> 2 [I > 2σ(I)]	0.1001
<i>R</i> 1(all data)	0.0685
<i>wR</i> 2(all data)	0.1124
largest diff. peak and hole [e Å ⁻³]	0.405/-0.467

Table S4. The specific parameters of hydrogen bonds of HGI-1.

Donor-H···Acceptor	D-H (Å)	H···A (Å)	D···A (Å)	\angle D-H···A (°)
N(1)-H(1A)···O(2)	0.88	2.26	2.594(3)	103
N(1)-H(1A)···O(4)	0.88	2.11	2.822(3)	137
N(1)-H(1B)···O(1)	0.88	2.29	2.625(3)	102
N(1)-H(1B)···O(5)	0.88	2.02	2.834(5)	152
N(2)-H(2A)···O(1)	0.88	2.24	2.610(3)	105
N(2)-H(2A)···O(2)	0.88	1.92	2.716(3)	149
N(2)-H(2B)···O(3)	0.88	2.01	2.618(3)	125
N(2)-H(2B)···O(3)	0.88	2.30	3.133(3)	158
N(4)-H(4A)···O(4)	0.85(3)	2.03(3)	2.609(3)	125(2)
N(4)-H(4A)···O(5)	0.85(3)	2.43(3)	3.119(5)	140(2)
N(4)-H(4B)···O(2)	0.90(3)	2.21(3)	2.593(3)	105(2)
N(4)-H(4B)···O(1)	0.90(3)	1.94(3)	2.757(3)	150(3)

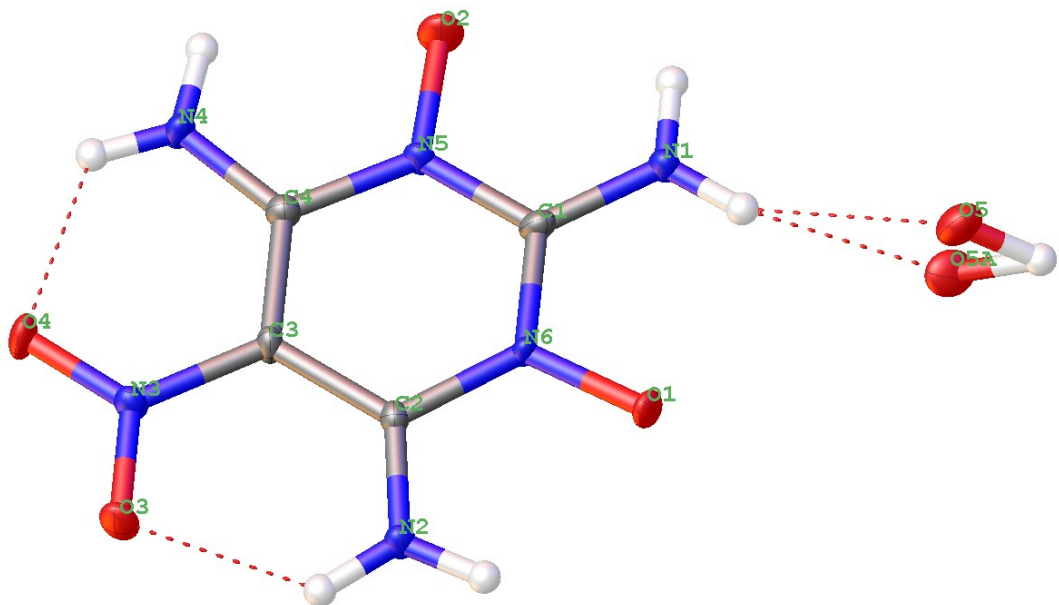


Table S5. The specific parameters of hydrogen bonds of HGI-2.

Donor-H···Acceptor	D-H (Å)	H···A (Å)	D···A (Å)	\angle D-H···A (°)
N(2)-H(2A)···O(3)	0.88(4)	2.20(3)	2.582(3)	106(3)
N(2)-H(2A)···O(1)	0.88(4)	2.59(3)	3.198(3)	127(3)
N(2)-H(2A)···O(2)	0.88(4)	2.59(4)	3.461(3)	169(2)
N(2)-H(2B)···O(2)	0.90(4)	1.94(4)	2.618(3)	130(3)
N(2)-H(2B)···O(6)	0.90(4)	2.57(3)	3.212(3)	129(3)
N(2)-H(2B)···O(7)	0.90(4)	2.43(4)	3.149(3)	137(3)
N(2)-H(2B)···N(1)	0.90(4)	2.57(4)	2.924(3)	104(2)
O(4)-H(4)···O(5)	0.84(4)	1.77(4)	2.601(3)	169(4)
N(4)-H(4A)···O(4)	0.87(2)	2.39(4)	2.681(3)	100(3)
N(4)-H(4A)···N(6)	0.87(2)	2.39(4)	2.843(3)	113(4)
N(4)-H(4B)···O(3)	0.86(2)	2.35(4)	2.654(3)	101(2)
N(6)-H(6A)···O(4)	0.82(2)	2.20(3)	2.552(3)	106(3)
N(6)-H(6A)···N(4)	0.82(2)	2.14(3)	2.843(3)	143(3)
N(6)-H(6B)···O(1)	0.90(4)	1.94(3)	2.597(3)	129(3)
N(6)-H(6B)···N(1)	0.90(4)	2.59(3)	2.907(3)	102(2)
N(6)-H(6B)···O(5)	0.90(4)	2.28(3)	3.041(3)	142(3)

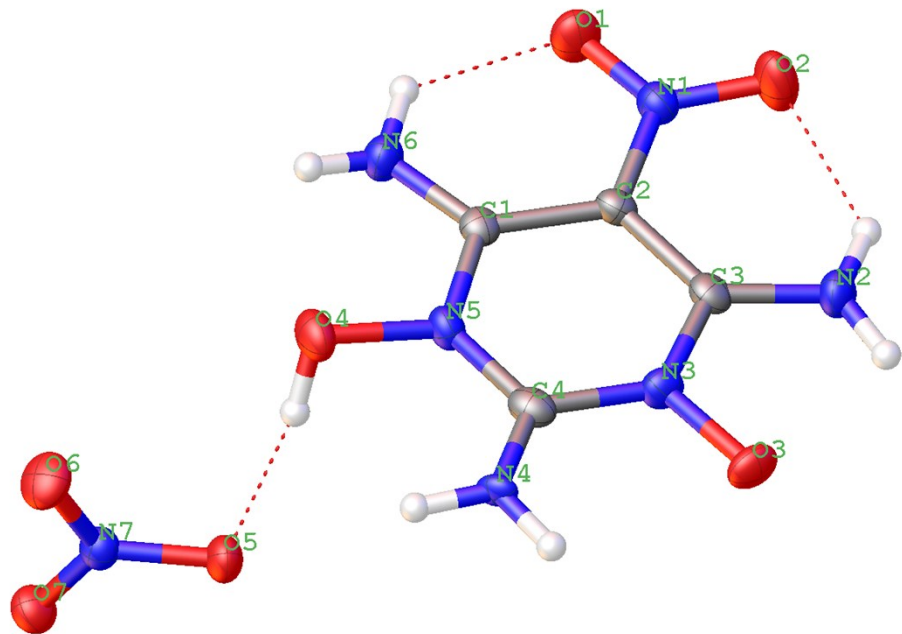
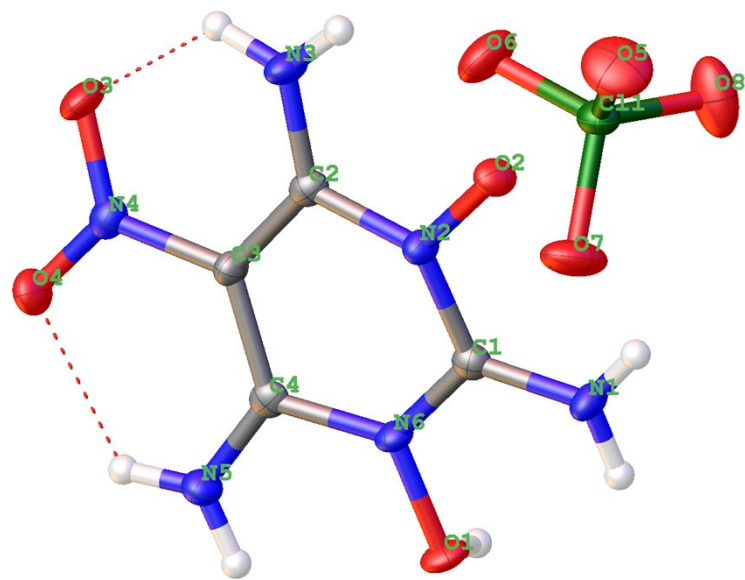


Table S6. The specific parameters of hydrogen bonds of HGI-3.

Donor-H···Acceptor	D-H (Å)	H···A (Å)	D···A (Å)	∠ D-H···A (°)
O(1)-H(1)···O(2)	0.87(3)	1.59(3)	2.465(3)	175(3)
O(1)-H(1)···N(2)	0.87(3)	2.44(3)	3.180(3)	144(3)
N(1)-H(1A)···O(2)	0.86	2.33	2.653(3)	102
N(1)-H(1A)···O(7)	0.86	2.09	2.952(3)	175
N(1)-H(1B)···O(1)	0.86	2.32	2.642(3)	103
N(1)-H(1B)···O(6)	0.86	2.10	2.905(3)	155
N(3)-H(3A)···O(2)	0.86	2.21	2.591(3)	106
N(3)-H(3A)···O(2)	0.86	2.18	2.824(3)	131
N(3)-H(3A)···O(5)	0.86	2.46	3.160(3)	138
N(3)-H(3B)···O(3)	0.86	2.01	2.598(3)	125
N(3)-H(3B)···O(7)	0.86	2.48	3.057(3)	125
N(5)-H(5A)···O(1)	0.86	2.27	2.636(3)	106
N(5)-H(5A)···O(8)	0.86	2.57	3.036(3)	115
N(5)-H(5A)···O(3)	0.86	2.26	2.842(3)	125
N(5)-H(5B)···O(4)	0.86	2.02	2.616(3)	126



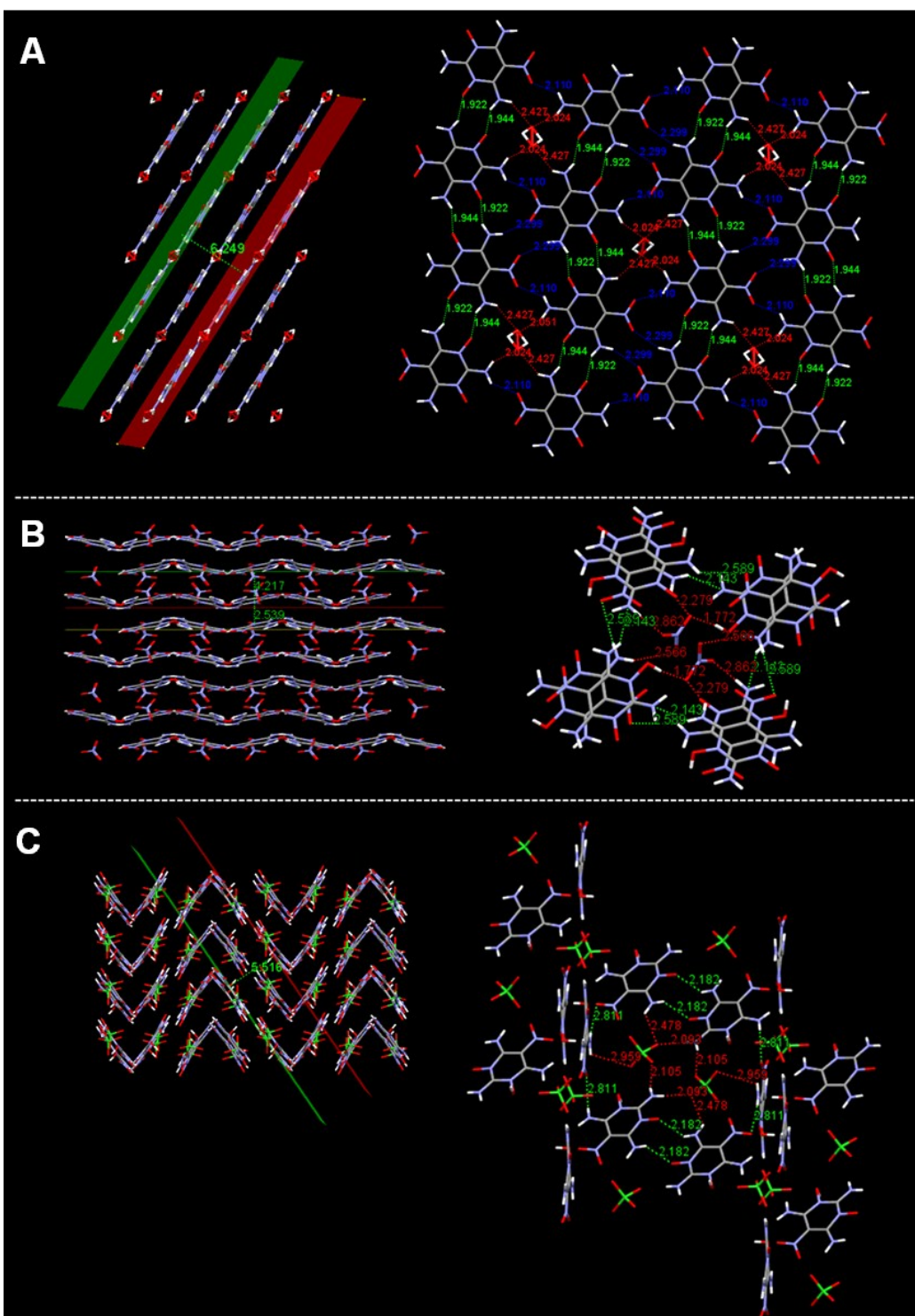


Figure S2. Crystal structural analysis on HGI-1, HGI-2 and HGI-3. (A) Interlamellar spacing and hydrogen bonds in the 2D molecular sheet in HGI-1 crystal. (B) Interlamellar spacing and hydrogen bonds in the 2D molecular sheet in HGI-2 crystal. (C) Interlamellar spacing and hydrogen bonds in the 2D molecular sheet in HGI-3 crystal.

Table S7. Physical properties of HGI-1, HGI-2, HGI-3 and the comparison with FOX-7, RDX, HMX and ε -CL-20.

	T_d^a (°C)	ρ^b (g cm ⁻³)	$\Delta_fH_m^c$ (kJ mol ⁻¹)	P^d (GPa)	v_D^e (m s ⁻¹)	IS ^f (J)	FS ^g (N)	OB ^h (%)
HGI-1	186	1.915 ⁱ	-40.3	34.8	9124	24	>360	-47.5
HGI-2	177	1.955 ^j	-56.15	39.1	9251	8	168	-27.2
HGI-3	233	1.995 ^j	1.24	42.5	9495	14	216	-15.9
FOX-7	220	1.88	-118.9	35.9	9000	24.7	>360	-21.6
RDX	210	1.80	86.3	34.9	8795	7.5	120	-21.6
HMX	279	1.90	116.1	39.2	9144	7.5	120	-21.7
ε -CL-20	215	2.04	365.4	46.7	9445	4	48	-11.0

^a) Onset decomposition temperature; ^b) Measured density by using a gas pycnometer at 298 K; ^c) Heat of formation; ^d) Detonation pressure calculated by using EXPLO5/6.02; ^e) Detonation velocity calculated by using EXPLO5/6.02; ^f) Impact sensitivity evaluated by a standard BAM fall-hammer method; ^g) Friction sensitivity evaluated by a BAM friction tester; ^h) Oxygen balance based on CO₂ for C_aH_bN_cO_dCl_e: OB (%) =1600×(d-a-(b-e)/2)/Mw. ⁱ) Crystal density at 100 K; ^j) Crystal density at 173 K.

The theoretical calculations on the solid-state heat of formation of HGI-1, HGI-2 and HGI-3. Because these three host-guest inclusion materials all contain two components (ICM-102 and the corresponding oxidant molecules) in their crystals, we consider them as a whole system to calculate their solid heat of formations (Δ_fH). Detailed calculation processes are presented by the following example of HGI-1.

Theoretical calculations were performed by using the Gaussian 09 (Revision D.01) suite of scripts². The geometric optimization and frequency analyses were completed by using the B3LYP functional with the 6-31+G** basis set. Single energy points were calculated at the MP2/6-31++G** level of theory. For all of the compounds, the optimized structures were characterized to be true local energy minima on the potential-energy surface without imaginary frequencies. The isodesmic reaction was carried out to obtain the gas-phase heat of formation of molecule ICM-102 (Fig. S3A). The gas-phase enthalpies of the building-block molecules were obtained by using the atomization method with the G2 ab initio calculations. For HGI-1, the solid-state heat of formation (HOF, Δ_fH°) was calculated based on a Born–Haber energy cycle³ (Fig. S3B) with following simplified calculation Equation:

$$\Delta_fH^\circ(\text{HGI-1, 298K}) = \Delta_fH^\circ(\text{HGI-1, 298K}) + 0.5\Delta_fH^\circ(\text{H}_2\text{O}_2, 298\text{K}) - \Delta H_{\text{sub}}$$

The heat of sublimation can be estimated using the DFT method with the GGA-RPBE (revised Perdew-Burke-Ernzerhof) exchange-correlation functional in Dmol3 program⁴⁻⁵.

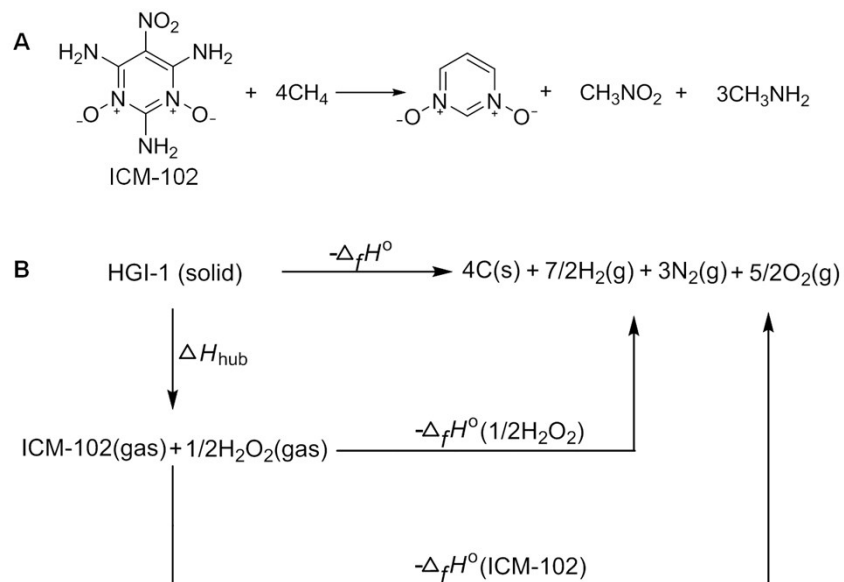


Fig. S3. Theoretical calculations on the solid-state heat of formation of HGI-1. (A) Isodesmic reaction of molecule ICM-102. (B) Born–Haber cycle for the formation of HGI-1.

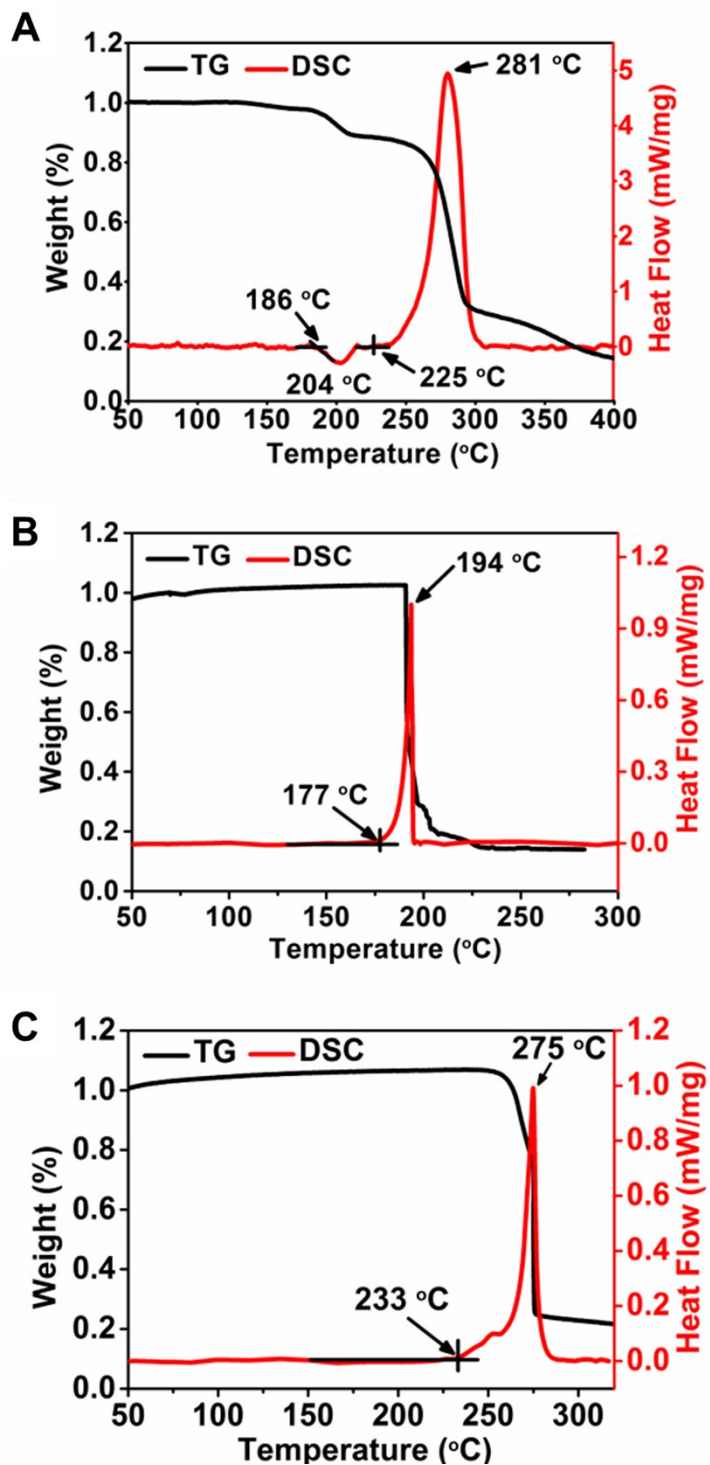


Fig. S4. Thermogravimetry (TG) and differential scanning calorimetry (DSC) curves of HGI-1, HGI-2 and HGI-3. (A) Thermogravimetry (TG) and differential scanning calorimetry (DSC) curves of HGI-1. (B) Thermogravimetry (TG) and differential scanning calorimetry (DSC) curves of HGI-2. (C) Thermogravimetry (TG) and differential scanning calorimetry (DSC) curves of HGI-3.

Table S8. Effect of replacing ammonium perchlorate (AP) with HGI-3 on the energy characteristics of GAP (GAP 10 % / Al 5 % / AP 60 % / RDX 25 %) propellant⁶.

GAP (%)	Al (%)	AP (%)	RDX (%)	HGI-3 (%)	$I_{sp}/(N\ s\ kg^{-1})$	$C^*/(m\ s^{-1})$	T _c /K	M _c
10	5	60	25	0	2568.35	1477.7	3359.9	25.88
10	5	55	25	5	2583.45	1491.3	3389.4	25.68
10	5	50	25	10	2593.06	1504.8	3410.8	25.47
10	5	45	25	15	2599.24	1517.1	3425.2	25.25
10	5	40	25	20	2602.77	1528.1	3432.9	25.01
10	5	35	25	25	2604.34	1537.7	3434.6	24.76
10	5	30	25	30	2604.24	1546.0	3430.7	24.51
10	5	25	25	35	2602.77	1553.1	3421.5	24.25
10	5	20	25	40	2600.22	1558.9	3407.8	23.98
10	5	15	25	45	2596.49	1563.6	3389.5	23.72

References

1. Cox, J. D.; Wagman, D. D.; Medvedev, V. A. *CODATA Key Values for Thermodynamics*, Hemisphere Publishing Corp, New York, **1989**.
2. Frisch, M. J. *et al.* Gaussian 09, Revision A.01; Gaussian, Inc.: Wallingford, CT, **2009**.
3. Cox, J. D.; Wagman, D. D.; Medvedev, V. A. *CODATA Key Values for Thermodynamics*, Hemisphere Publishing Corp, New York, **1989**.
4. B. Delley, *J. Chem. Phys.* 1990, **92**, 508-517.
5. B. Delley, *J. Chem. Phys.* 2000, **113**, 7756-7764.
6. M. Li, F. -Q. Zhao, Y. Luo, S. -Y. Xu and E. -G. Yao, *Chin. J. Energy Mater.*, 2014, **22**, 286-290.